Interaction of soil water and groundwater during the freezing-thawing cycle: field observations and numerical modeling

Hong-Yu Xie[1], Xiao-Wei Jiang[1*], Shu-Cong Tan[1], Li Wan[1], Xu-Sheng Wang[1], Yijian Zeng[2]

1. MOE (Ministry of Education) Key Laboratory of Groundwater Circulation and Evolution, China University of Geosciences, Beijing 100083, China

2. Department of Water Resources, ITC Faculty of Geo-Information Science and Earth Observation, University of Twente, Enschede, the Netherlands

*Correspondence to: Xiao-Wei Jiang (jxw@cugb.edu.cn)

Abstract

Freezing-induced ~~water migration and~~ groundwater level decline are widely observed in regions with shallow water table, but many existing studies trying to quantify freezing-induced groundwater migration do not account for water level fluctuations induced by freezing and thawing. Here, detailed field observations of liquid soil water content and groundwater level fluctuations at a site in the Ordos Plateau, China are combined with numerical modeling to show groundwater and soil water dynamics controlled by wintertime atmospheric conditions and topographically-driven lateral groundwater inflow. At the field site where the initial water table depth is around 120 cm and the lateral groundwater inflow rate is fitted to be 1.03 mm/d, the observed fluctuating soil water contents and groundwater level induced by freezing and thawing are well reproduced. By calculating the budget of groundwater, the mean upward flux of freezing-induced groundwater loss is 1.46 mm/d for 93 days, ~~and~~ while the mean flux of thawing-induced groundwater gain is as high as 3.94 mm/d for 32 days, which can be useful for future studies on two- or three-dimensional transient groundwater flow in semi-arid regions with seasonally frozen soils. By comparing models under a series of conditions, we found the magnitude of freezing-induced groundwater loss decreases with initial water table depth and increases with the rate of groundwater inflow. We also found a fixed-head lower boundary condition would overestimate freezing-induced groundwater migration when the water table depth is shallow. Therefore, an accurate characterization of freezing-induced water table

decline is critical to quantifying the contribution of groundwater to hydrological and ecological processes in cold regions.~~lateral groundwater inflow leads to an alleviated freezing-induced groundwater level decline and enhanced freezing-induced water migration. At the field site with a lateral groundwater inflow rate of 1.03 mm/d, compared with the case without lateral groundwater inflow, the water level decline decreases from 40 cm to 15 cm, and the increased total water content in the frozen zone enhances from 0.071 to 0.106. The study enhances our understanding of the mechanisms controlling water redistribution between saturated and unsaturated zones and the water budget in the freezing-thawing cycle. The fluxes of groundwater loss and gain in the freezing and thawing stages obtained in the current study can be useful for future studies on two- or three-dimensional transient groundwater flow in semi-arid regions with seasonally frozen soils~~

1 Introduction

Frozen soils, which can be divided into permafrost and seasonally frozen soils, have great impacts on many hydrological, hydrogeological processes and ecological processes (Nelson, 2003;Kurylyk et al., 2014;Schuur et al., 2015;Walvoord and Kurylyk, 2016;Evans et al., 2018). ~~In fact, frozen soils can be divided into permafrost and seasonally frozen soils, which underlie approximately 26% and 24%, respectively, of the Northern Hemisphere exposed land surface (Zhang et al., 2003;Dobinski, 2011;Evans and Ge, 2017).~~ In seasonally frozen soils, ~~The~~ the behaviors of subsurface water flow and storage ~~in seasonally frozen soils~~ are distinct from those in ~~both~~ colder regions with permafrost and as well as in warmer regions with insignificant frozen soil (Ireson et al., 2013). Understanding the effects of soil freezing and thawing on subsurface water flow and storage is a necessary path for better water resources management in ~~(semi-)arid~~ regions with occurrence of seasonally frozen soils (Yu et al., 2020).

In seasonally frozen regions, by blocking pores and reducing hydraulic conductivity, soil freezing could lead to decreased infiltration (van der Kamp et al., 2003;Iwata et al., 2008;Demand et al., 2019) and limited surface evaporation (Kaneko et al., 2006;Wu et al., 2016). As a result of cryosuction generated by s~~S~~oil freezing, ~~also generated cryosuction~~ (Williams and Smith, 1989;Hohmann, 1997;Yu et al., 2018), ~~which causes migration of~~ water from the unfrozen zone would migrate to the freezing front ~~and further decrease the hydraulic conductivity of frozen soils~~. By assuming that freezing-induced water migration is restricted within the shallow part of unsaturated zone ~~which is~~ far away from the water table, many numerical studies deployed a free drainage lower boundary condition and examined the effects of freezing-induced water redistribution on infiltration and runoff (Cherkauer and Lettenmaier, 1999;Okkonen et al., 2017;Zhang et al., 2017). In fact, groundwater in the saturated

zone can also be migrated freezing-induced water movement is not restricted within the unsaturated zoneto the freezing front (Harlan, 1973;Shoop and Bigl, 1997;Stähli et al., 1999;Hansson and Lundin, 2006;Ireson et al., 2013;Chen et al., 2019), especially in regions with shallow groundwater, which widely occur in topographic lows (Gleeson et al., 2011;Fan et al., 2013). Although there are many field observations of freezing-induced groundwater level decline since the 1950s (Drescher, 1955;Schneider, 1961;Daniel and Staricka, 2000;van der Kamp et al., 2003;Ireson et al., 2013;Zhang et al., 2019), numerical research on freezing-induced water redistribution that satisfactorily considers freezing-induced groundwater level decline is limited.

Freezing-induced water migration from the saturated zone to the freezing front would necessarily strengthen the possibility of frost heave (Chamberlain, 1981;Bronfenbrener and Bronfenbrener, 2010;Rui et al., 2019). During the thawing stage, accumulation of thawed water above the frozen zone would accelerate soil evaporation (Fetzer et al., 2017;Vanderborgh et al., 2017;Li et al., 2020), which is critical to soil salinization (Liu et al., 2009;Lopez et al., 2010;Bechtold et al., 2011). Therefore, Tthe amount of freezing-induced water migration from the saturated zone to the frozen zone is key to understanding the effects of soil freezing on engineering problems hydrogeological and ecologicalecohydrological processes and engineering problems, a key knowledge is the amount of freezing-induced water migration from the saturated zone to the frozen zone. In some previous experimental and numerical studies, freezing-induced water migration from groundwater to the frozen zone was obtained by assuming a fixed water table (Shoop and Bigl, 1997;Hansson and Lundin, 2006;Alkhaier et al., 2012;Chen et al., 2019). It was found that a fixed head lower boundary condition, even if the fixed head is close enough to the mean water table, would overestimate groundwater loss to support evapotranspiration Because because a fixed water tablesuch a boundary condition implies that loss of groundwater can be replenished instantaneously (Zhu et al., 2009)., such a model would overestimate freezing-induced water migration from groundwater. However, the degree of overestimation of freezing-induced water migration by using a fixed head lower boundary condition remains unknown.

As initially proposed by Hubert (1940) and Tóth (1962), lateral groundwater flow is ubiquitous in regions with undulating topography and water table. Although wintertime water table fluctuations caused by freezing and thawing have been widely recognized (Willis et al., 1964;van der Kamp et al., 2003;Zhang et al., 2019), the simultaneous contribution of lateral groundwater flow to wintertime water table fluctuations received little attention. Ireson et al. (2013) found the wintertime water table recessions in their two study sites in the Canadian prairies were partly due to lateral groundwater outflow, while Jiang et al. (2017) found the pattern of wintertime water table fall-rise in their study site in the Ordos Plateau, China was also influenced by lateral groundwater

inflow. Therefore, the wintertime water table dynamics ~~is not prior known, but is a function of~~ should be a part of model output ~~both~~ induced by atmospheric conditions and lateral groundwater inflow/outflow, instead of ~~and~~ a prior known boundary condition~~should be a part of model output~~. To obtain a clear understanding of wintertime water migration and water budget in regions with shallow groundwater, it is appealing to numerically combine hydrological processes in both saturated and unsaturated zones, including topographically-driven lateral flow in the saturated zone, freezing-induced water migration from the saturated to the unsaturated zone, and thawing-induced water movement. In the current study, the field site reported in Jiang et al. (2017), which has shallow water table and lateral groundwater inflow, is used as an example, and a series of scenarios with different water table depths and lateral groundwater inflow rates are used to numerically examine the interactions of soil water and groundwater ~~and calculate the water budget during the freezing-thawing cycle~~.

2 Methods

2.1 Study area and conceptual model

The Ordos Plateau in Northwestern China has a semi-arid and ~~cold~~seasonally-frozen climate, and is ~~one of the most intensively studied groundwater basins~~well-known for the occurrence of topography-driven regional groundwater flow ~~due to its dependence on groundwater~~ (Hou et al., 2010;Jiang et al., 2018). The main aquifer is the thick Cretaceous sandstone, which is overlain by a thin layer of sand ~~Quaternary sediments~~. Due to the spatially undulating topography and low permeability of the sandstone aquifer, water table undulation is a subdued replica of the topography and regional groundwater generally flows laterally from topographic highs to topographic lows of a catchment. In a specific catchment, as a result of the ~~occurrence of a small lake in topographic lows and the~~ contribution of lateral groundwater flow from topographic highs towards the lake ~~in the lowest discharge point~~, water table is shallow in topographic lows near the lake. The Wudu Lake catchment (Wang et al., 2015; Zhao et al., 202~~0~~1) is one of the small catchments located to the southeast of the first-order water divide of the Ordos Plateau. Based on measurements of 53 wells in the catchment (the location of wells can be found in Jiang et al. ~~(~~, 2018)~~)~~, water table depth increases from less than 0.5 m in topographic lows to 26.1 m near the divide ~~while the zone of flowing wells, i.e., with higher hydraulic head than the topography, can be found in Wang et al. (2015)~~. In topographic lows with water table ranges between around 1 m to 2 m, the typical vegetation is *Achnatherum splendens*.

The Otak meteorological station, which is a national meteorological station, is around 35 km away from the center of the Wudu Lake catchment. ~~According to the meteorological data in the Otak station f~~From 1955 to 2016

(data ~~from China Meteorological Data Service Center,~~ available at http://data.cma.cn), the annual mean precipitation is 265.0 mm, including an annual mean snowfall of 16.0 mm, and the annual mean pan evaporation is 1370.0 mm. Note that the amount of snowfall is determined by weighting water equivalent of snowfall, and the accuracy of precipitation and pan evaporation measurements is ±0.1 mm. July has the largest monthly mean temperature equaling 22.5 ℃ while January has the lowest monthly mean temperature equaling -10.4 ℃. The period from late November to late March corresponds to the freezing-thawing cycle. As shown in Jiang et al. (2018), freezing-induced groundwater level decline occurs in the monitoring well DK2 located in topographic lows, but does not occur in the monitoring well DK1 located in topographic highs. ~~Groundwater level declines induced by evapotranspiration in the summer and by freezing in the winter have been reported in some sites with shallow groundwater (Jiang et al., 2017;Zhang et al., 2019). The relationship between groundwater, soil water and the summertime atmospheric conditions, i.e., infiltration and evapotranspiration, has been numerically coupled by some researchers (Chen et al., 2019;Zhao et al., 2020). The average monthly temperature decreases from -1.5 ℃ in November to -10.4 ℃ in January and increases from -6.4 ℃ in February to 0.9 ℃ in March, therefore, the period from late November to late March corresponds to the freezing-thawing cycle. However, there is no numerical study on how groundwater and soil water dynamics respond to wintertime atmospheric conditions.~~

In the Wudu lake catchment, the occurrence of numerous flowing wells in topographic lows indicates an upward hydraulic gradient (Wang et al., 2015), which also induces groundwater inflow into the shallow part of the aquifer. At the monitoring site, lateral groundwater flow had been found to be an indispensable component of groundwater budget (Jiang et al., 2017). Fig. ~~2~~ 1 shows the control of main hydrological and hydrogeological processes on groundwater level during the freezing-thawing cycle. The processes leading to water level decline include water migration induced by freezing and evaporation due to the cold and dry climate, and the processes leading to water level rise is lateral groundwater inflow throughout the whole ~~cycle~~ period and infiltration of thawed water during the thawing stage.

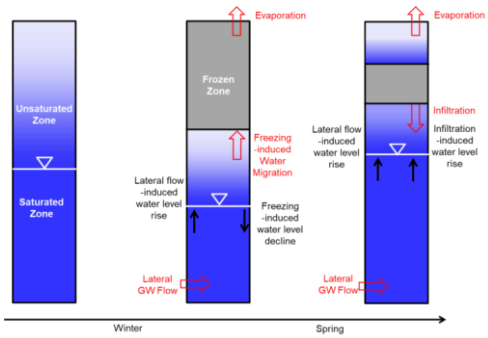

Figure ~~2~~ 1 The conceptual model~~s~~ of hydrological processes and groundwater regime in semi-arid regions during the ~~seasonally~~ freezing ~~and~~ thawing ~~stages~~cycle.

2.2 Field measurement

To examine how atmospheric conditions control groundwater dynamics in topographic lows, we set up a monitoring profile of soil water contents and soil temperatures adjacent to the groundwater level monitoring well DK2. ~~There is a monitoring site of soil water content and groundwater level in the topographic lows of this catchment. The water table depths are recorded by using water level loggers in a shallow well with a depth of 10 m while the~~Soil temperatures and liquid water contents in the Quaternary ~~deposits~~ sands are recorded at 8 depths (at around 10 cm, 20 cm, 30 cm, 50 cm, 70 cm, 90 cm, 110 cm, 150 cm below surface) by using 5TM sensors produced by Decagon Devices ~~at 8 depths (at around 10 cm, 20 cm, 30 cm, 50 cm, 70 cm, 90 cm, 110 cm, 150 cm)~~. The 5TM sensors, which measure the soil dielectric permittivity to represent liquid soil water content, have an accuracy of around ±2% volumetric water content and a resolution of 0.001 cm^3/cm^3. To insure the representativeness of measurement, we performed site-specific calibration by comparing the liquid water content measured by the 5TM sensors and by the gravimetric method. It has been reported that 5TM sensors are accurate enough to measure the liquid water content even if soil is partially frozen (Yang et al., 2013; Xue et al., 2021).

~~At the monitoring site, lateral groundwater flow had been found to be an indispensable component of groundwater budget . Fig. 2 shows the control of main hydrological and hydrogeological processes on groundwater level during the freezing-thawing cycle. The processes leading to water level decline include water migration induced by freezing and evaporation due to the dry climate, and the processes leading to water level rise is lateral groundwater flow throughout the cycle and infiltration of thawed water during the thawing stage.~~

To obtain the bulk density, ~~We collected~~ soil samples were collected by the cutting-ring method at 12 depths (at around 10 cm, 20 cm, 30 cm, 40 cm, 50 cm, 60 cm, 70 cm, 80 cm, 90 cm, 100 cm, 110 cm and 120 cm) ~~to obtain the bulk density~~. We also collected soil samples from the 12 depths for measuring soil particle size by

using the Mastersizer 2000 instrument (Malvern Instruments, England). ~~The measured soil parameters are shown in the Table 1.~~ The saturated hydraulic conductivity of soil samples from selected layers were measured by HYPROP (www.metergroup.com/environment/products/hyprop-2/). The soil samples with low clay content above 70 cm and below 100 cm were measured to be around 43.2 m/d, while that with higher clay content at the depth ranging between 70 and 100 cm is measured to be 1.9 m/d.

In this study, the data collected during 28 NOV 2015 and 1 APR 2016 is used as an example. As shown in Fig. 2~~1~~, water table depth increases from 115 cm on 28 NOV 2015 to 143 cm on 29 JAN 2016, which corresponds to the stage with an increasing frost depth~~which is a direct result of freezing-induced water migration from groundwater to the freezing front~~.

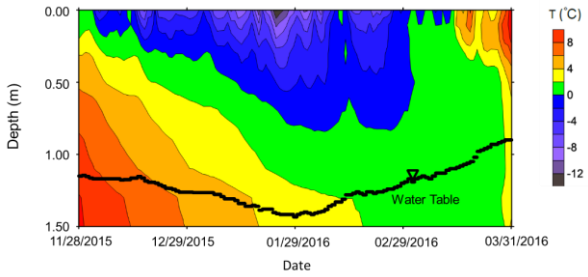

Figure ~~1~~2. The contour map ~~showing~~ shows the change of soil temperature at the study site during the freezing-thawing cycle. Also shown is the fluctuating groundwater level monitored at the study site.

2.3. The SHAW model

By assuming that the mechanisms of water transport in partially frozen soils are similar to those in unsaturated soils, Harlan (1973) pioneered modeling studies of heat-fluid transport with freezing-thawing by considering the co-existence of a frozen zone, an unsaturated unfrozen zone and a saturated unfrozen zone. The Simultaneous Heat and Water (SHAW) model (Flerchinger and Saxton, 1989) is one of the most robust Harlan-type models for freezing-induced water migration in the one-dimensional domain (Hayhoe,1994; DeGaetano et al., 2001;Kahimba et al., 2009; Li et al., 2010; Zhang et al., 2017). A one-dimensional soil column is justified to account for water redistribution induced by freezing and thawing because water flow in the unsaturated zone is predominantly vertical (Stephens, 1996;Romano et al., 1998;Van Dam and Feddes, 2000). The contributions of liquid water, ice, and vapor contents have been considered in the water balance equation, and the contributions of heat conduction, phase change, liquid flow, and vapor gas diffusion have been considered in the energy balance equation ~~(Li et al., 2010). Because water flow in the unsaturated zone is predominantly vertical (Stephens,~~

~~1996;Romano et al., 1998;Van Dam and Feddes, 2000), the SHAW model only accounts for the effects of soil freezing and thawing on water redistribution within a one-dimensional (1D) soil column. Moreover, b~~By adding a source term representing the flux of groundwater inflow/outflow in the water balance equation, it has the ability to simultaneously account for the contributions of lateral groundwater flow and freezing/thawing ~~to water level~~ in the soil column. Therefore, the SHAW model is suitable to couple the groundwater dynamics with soil water dynamics during the freezing-thawing cycle as observed in our field site.

Considering convective heat transfer by liquid, latent heat transfer by ice and latent heat transfer by vapor, the energy balance equation in the soil matrix is expressed as

$$C_s\frac{\partial T}{\partial t}-\rho_i L_f\frac{\partial \theta_i}{\partial t}=\frac{\partial}{\partial z}\left[k_T\frac{\partial T}{\partial z}\right]-\rho_l c_l\frac{\partial q_l T}{\partial z}-L_v\left[\frac{\partial q_v}{\partial z}+\frac{\partial \rho_v}{\partial t}\right] \quad (1)$$

where T is temperature [Θ], θ_i is volumetric ice content [-], z is soil depth [L], t is time [T], ρ_i, ρ_l and ρ_v are densities of ice, liquid water and vapor [M L^{-3}], respectively, L_f and L_v are latent heat of fusion and vaporization [L^2 T^{-2}], respectively, q_l is liquid water flux [L T^{-1}], q_v is water vapor flux [M L^{-2} T^{-1}], c_l is specific heat capacity of water [L^2 T^{-2} Θ^{-1}], C_s is volumetric heat capacity of soil [M L^{-2} T^{-2} Θ^{-1}], and k_T is thermal conductivity of soil [M L^2 T^{-3} Θ^{-1}]. ~~Calculation of C_s and k_T can be found in Flerchinger and Saxton (1989) and is not reproduced here.~~ C_s of soil is determined by the sum of the volumetric heat capacities of the soil constituents:

$$C_s=\sum \rho_j c_j \theta_j \quad (2)$$

域代码已更改

and k_T of soil is calculated by (De Vries, 1963)

$$k_T=\frac{\sum m_j k_j \theta_j}{\sum m_j \theta_j} \quad (3)$$

域代码已更改

where ρ_j, c_j , θ_j , k_j and m_j are the density, specific heat capacity, volumetric fraction, thermal conductivity and weighting factor of the j^{th} soil constituent (sand, silt, clay, water, ice and air).

By considering ice content change and vapor flux, the water balance equation is written as

$$\frac{\partial \theta_l}{\partial t}+\frac{\rho_i}{\rho_l}\frac{\partial \theta_i}{\partial t}=\frac{\partial}{\partial z}\left[K\left(\frac{\partial \psi}{\partial z}+1\right)\right]+\frac{1}{\rho_l}\frac{\partial q_v}{\partial z}+U \quad (~~2~~4)$$

where θ_l is liquid water content [-], K is hydraulic conductivity [L T^{-1}], ψ is soil matric potential [L], and U is a source/sink term for water flux [T^{-1}]. The lateral inflow rate per unit volume, which is one form of source, is calculated by using the Darcy's law based on a constant horizontal hydraulic gradient at selected nodes within the saturated zone. Soil water characteristic curves, which describe the relationship between soil matric potential and liquid water content, are defined for both unfrozen and frozen soils. Here, the van Genuchten equation (van

Genuchten, 1980) is selected, which is written as

$$\frac{\theta_l-\theta_r}{\theta_s-\theta_r}=\left(1+|\alpha\psi|^n\right)^{-m} \quad (35)$$

where θ_s and θ_r are saturated and residual water content [-], α [L^{-1}], n [-] and m [-] are empirical parameters. α equals the inverse of the air-entry value, n is a pore-size distribution index and m=1-1/n. In the frozen zone, due to the co-existence of liquid water and ice, matric potential is strongly dependent on temperature, and the matric potential is obtained by the following equation (Fuchs et al., 1978):

$$\psi=\frac{L_f}{g}\frac{T}{T+273.15} \quad (46)$$

where g is the acceleration of gravity [$L\ T^{-2}$]. Eq. (4) indicates that as the negative temperature increases, the soil suction also increases (matric potential becomes more negative).

In the unfrozen zone, ~~The~~ the hydraulic conductivity of ~~the unfrozen zone~~ is computed by

$$K=K_s S_e^l\left[1-\left(1-S_e^{1/m}\right)^m\right]^2 \quad (57)$$

where K_s is the saturated hydraulic conductivity [$L\ T^{-1}$], S_e [-] is the effective saturation calculated by $(\theta_l-\theta_r)/(\theta_s-\theta_r)$, and l [-] is a pore-connectivity parameter which is assumed to be 0.5 in the original work of (Mualem, 1976). ~~Note that in the saturated unfrozen zone, K equals K_s, but in the unsaturated unfrozen zone, K equals unsaturated hydraulic conductivity (K_u).~~ In the frozen zone, ~~due to~~ occupation of ice in the pores would decrease the available porosity and thus hydraulic conductivity. When the available porosity is lower than 0.13, K is assumed to be 0; when the available porosity is above 0.13, ~~the unsaturated hydraulic conductivity~~K computed from Eq. (57) is reduced linearly with ice content assuming zero conductivity at an available porosity of 0.13~~and is assumed to be zero when the porosity is decreased to 0.13~~ (Flerchinger, 2000).

The freezing-thawing cycle is usually accompanied by occasional or frequent snowfall events. In the SHAW model, precipitation is assumed to be snowfall if the air temperature is below 0℃ ~~and the depth of snowpack should be input~~. When snow falls on bare soil with a surface temperature of below 0 ℃, a snow cover layer is formed~~,~~. ~~t~~The energy balance for the snow cover is written as follows (Flerchinger, 2000):

$$\rho_{sp}c_i\frac{\partial T}{\partial t}+\rho_l L_f\frac{\partial w_{sp}}{\partial t}=\frac{\partial}{\partial z}\left[k_{sp}\frac{\partial T}{\partial z}\right]+\frac{\partial R_n}{\partial z}-L_s\left[\frac{\partial q_v}{\partial z}+\frac{\partial \rho_v}{\partial t}\right] \quad (8)$$

域代码已更改

where ρ_{sp} is the density of snow [$M\ L^{-3}$], w_{sp} is the liquid water content in the snow [-], c_i is heat capacities of ice [$L^2\ T^{-2}\ \Theta^{-1}$], L_s is latent heat of sublimation [$L^2\ T^{-2}$], k_{sp} is thermal conductivity of snow [$M\ L^2\ T^{-3}\ \Theta^{-1}$], R_n is the net downward radiation flux within the snow [$M\ L^2\ T^{-4}$]. In the SHAW model, if the air temperature is increased to above 0℃, snow got melted~~, which could infiltrate into the subsurface~~. Snowmelt in excess of the calculated

interception could infiltrate into the subsurface medium when the maximum depth of ponding is set to be a positive value.

2.4. Model inputs

In the following, based on the conceptual model shown in Figure 21, we use SHAW to couple observed soil water and groundwater dynamics ~~in a 1D soil column~~ during the freezing-thawing cycle from 28 NOV 2015 to 1 APR 2016, as such to understand how the coupled unsaturated-saturated processes respond to wintertime atmospheric conditions. The time step of simulations is one hour. Because the deepest water table depth is 143 cm and soil temperature at 150 cm below surface is available, ~~To ensure that the lateral groundwater inflow occurs within the saturated zone,~~ the length of the 1D soil column is set to be 150 cm. The model domain is uniformly divided into ~~31~~ 30 layers, which results in ~~32~~ 31 nodes. The stable variables of the model include soil temperature and soil water content. The top node has an atmospheric boundary condition, while the bottom node has a zero-flux and specified-temperature boundary condition. ~~Following Flerchinger (2000), t~~The occurrence of lateral groundwater flow is realized by ~~setting a specified~~ specifying a hydraulic gradient at a node within the saturated zone ~~the last but one node (31st~~ the 30th node in the current study). In this way, the ~~fluctuation~~ fluctuating ~~of~~ groundwater level is an outcome of wintertime atmospheric conditions and lateral groundwater flow, while the fluctuating ~~fluctuations of~~ soil water content ~~are~~ is controlled by both wintertime atmospheric conditions and groundwater dynamics.

The inputs for the atmospheric boundary conditions include maximum air temperature, minimum air temperature, wind speed, precipitation, solar radiation and dew-point temperature. The first four parameters are available from the observations at the Otak meteorological stations, the parameter of solar radiation is calculated by the Angström-Prescott equation (Yorukoglu and Celik, 2006) based on the sunshine duration ~~(data available at http://data.cma.cndata available from China Meteorological Data Service Center)~~, and the dew-point temperature is calculated by the Hyland-Wexter equation (Wexler et al., 1983) based on relative humidity, maximum air temperature and minimum air temperature. Fig. 3 shows the maximum and minimum air temperatures, dew-point temperature and precipitation. The inputs for the lower boundary condition at the bottom include a zero hydraulic conductivity to insure a no-flux boundary condition, and the daily averaged soil temperature measured at ~~approximately corresponding depth~~150 cm below surface for the specified-temperature boundary condition. The initial conditions of soil water content and soil temperature for spin-up are determined based on measured values

on 29 OCT 2015, and ~~T~~the model spin-up is run for 30 days before the start of freezing time (28 NOV 2015). ~~to reach a quasi-steady state. , i.e., the~~The initial conditions of soil water content and soil temperature for spin-up ~~are determined based on measured values on 29 OCT 2015~~.

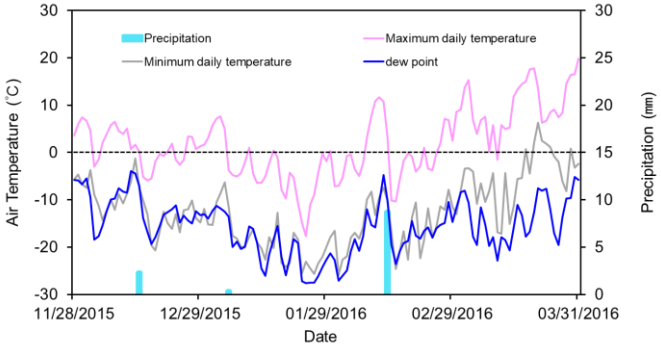

Figure 3 the maximum daily air temperature, the minimum air temperature, dew-point temperature and precipitation during the freezing-thawing cycle from 28 NOV 2015 to 1 APR 2016.

~~Although soil samples from all depths belong to sand or loamy sand, s~~Soil texture determines the thermal parameters and the initial hydraulic parameters~~, note that, the hydraulic parameters and the lateral groundwater inflow should be further calibrated by fitting the simulated and measured soil water content and water table depth~~. As shown in Table 1, The percentage of clay ranges between 5 and 8% in the layer between 70 and 100 cm, and between 1 and 4% in other depths ~~(Zhao et al., 2020)~~. Therefore, the model domain is divided into three layers. Based on average contents of clay, silt and sand in each layer, the thermal parameters are calculated by using equations (2) and (3).~~The parameters for the van Genuchten (1980) and Mualem (1976) models obtained by Zhao et al. (2020)~~ and the hydraulic parameters (θ_r, θ_s, α, n) are initially estimated by the Rosetta pedotransfer function (Schaap and Leij 1998; Zhang and Schaap 2017) and are further calibrated to fit the measured liquid soil water content, which are shown in Table ~~1~~2. ~~As shown in Table 2, the further calibrated parameters result in much lower RMSEs.~~ Based on the possible range of lateral inflow rate varying between 0.96 and 1.16 mm/d (Jiang et al., 2017), the lateral inflow rate is calibrated to be 1.03 mm/d, which leads to the lowest RMSE of water table depth. ~~This base case is denoted as Scenario A in Sect. 3.2.~~

Table 1 The mearsured soil texture and bulk density.

Depth (cm)	Clay (%)	Silt (%)	Sand (%)	Bulk density (g/cm^3)
10	1.5	9.4	89.1	1.638

20	1.6	9.5	88.9	1.673
30	1.5	9.5	89.0	1.628
40	2.0	9.5	88.5	1.672
50	2.5	9.1	88.3	1.655
60	2.7	9.7	87.6	1.613
70	5.5	13.5	81.0	1.562
80	6.4	11.2	82.4	1.518
90	6.1	9.2	84.7	1.549
100	7.7	10.4	81.9	1.598
110	3.0	9.4	87.6	1.652
120	1.7	9.7	88.6	1.733

Table 2 Calibrated hydraulic parameters for the van Genuchten (1980) and Mualem (1976) models.

Depth (m)	θ_r ($m^3 m^{-3}$)	θ_s ($m^3 m^{-3}$)	α (m^{-1})	n (-)	K_s ($m\ d^{-1}$)
0 - 0.7	0.012	0.408	4.1	2.06	3.84
0.7 - 1.0	0.076	0.381	3.6	1.86	0.41
1.0 -1.5	0.032	0.403	6.4	2.26	3.41

To examine the role of lateral groundwater inflow and water table depth ~~soil heterogeneity~~ in freezing-induced groundwater migration, we build different scenarios with ~~four~~three different initial water table depths (120 cm, 170 cm, and 220 cm~~, and 250 cm~~) and three different lateral flow rates (0, 0.51 mm/d, and 1.03 mm/d) for sensitivity analysis. We also build one scenario with an initial water table depth of 250 cm but without lateral groundwater inflow, and three scenarios with water table depths fixed at 120 cm, 170 cm, and 220 cm. The specific settings of the 13 scenarios are shown in Table 3. To insure that water table can be explicitly represented in the models, the length of model domain is extended to be 250 cm. To exclude the influence of heterogeneity, the whole soil column is assumed to be filled with sand of ~~we assume the whole soil column has~~ the same soil texture as that of 0 cm to 70 cm in the ~~base case~~field site.~~, and all other conditions are kept unchanged as Scenario A. By setting the lateral inflow rate to be zero, Scenario A changes into Scenario C and Scenario B changes into Scenario D. Because the disappearance of lateral groundwater inflow would lead to much deeper water table depth, the length of the 1D soil column in~~

~~Scenarios C and D is extended to 200 cm. In Scenario C, the layer from 155 cm to 200 cm is assumed to have the same soil texture as that from 100 cm to 155 cm.~~ Because there is no temperature measurement at 250 cm below surface, ~~the temperature at the lower boundary is estimated by the method proposed by Hirota (2002), which is based on heat conduction and energy balance.~~the temperature at the lower boundary is estimated by the force-restore approach embedded in the SHAW model, which can be written as (Hirota et al., 2002):

$$\left(1+\frac{2z}{d_d}\right)\frac{\partial T}{\partial t}=\frac{2}{C_s d_d}G-\omega\left(T-T_{AVG}\right) \quad (9)$$

where z is the depth [L] below the surface, ω is the frequency [T^{-1}] of fluctuation period, d_d is damping depth [L] corresponding to ω, which is expressed as $d_d=\left(\frac{2k_T}{C_s\omega}\right)^{1/2}$, and T_{AVG} is the average annual air temperature [Θ].

Table 3 The different scenarios of sensitivity analysis with different initial water table depths and different conditions of groundwater supply.

Scenarios	Initial Water Table Depth (cm)	Groundwater supply
Scenario A1	120	LFR*=0
Scenario A2	120	LFR=0.51 mm/d
Scenario A3	120	LFR=1.03 mm/d
Scenario A4	120	Determined by the fixed water table
Scenario B1	170	LFR=0
Scenario B2	170	LFR=0.51 mm/d
Scenario B3	170	LFR=1.03 mm/d
Scenario B4	170	Determined by the fixed water table
Scenario C1	220	LFR=0
Scenario C2	220	LFR=0.51 mm/d
Scenario C3	220	LFR=1.03 mm/d
Scenario C4	220	Determined by the fixed water table
Scenario D	250	LFR=0

*LFR represents lateral flow rate.

~~Table 2 The RMSEs of simulated liquid water content obtained with different parameters~~

~~Parameters~~	~~10 cm~~	~~20 cm~~	~~30 cm~~	~~50 cm~~	~~70cm~~
~~Calibrated parameters~~	~~0.0213~~	~~0.0205~~	~~0.0289~~	~~0.0175~~	~~0.0231~~

域代码已更改

域代码已更改

~~Initial parameters~~	~~0.0485~~	~~0.0512~~	~~0.0553~~	~~0.0432~~	~~0.0427~~

3 Results and discussion

3.1 Field data showing freezing-induced water migration and water level decline

The contour with temperature equaling 0 ℃ shown in Fig. 2 well characterizes the gradual deepening of frost depth during the freezing stage from 28 NOV 2015 to 29 FEB 2016, but soil temperature is not enough to demonstrate freezing-induced water migration. Fig. 4 shows the evolutions of liquid water content and soil temperature at 6 depths ~~general trend of deepening frost depth~~ (10 cm, 20 cm, 30 cm, 50 cm, 70 cm, and 90 cm, ~~Fig. 1~~). The dates of the start of freezing, i.e., when soil temperature drops to 0 ℃, at 10 cm, 20 cm, 30 cm, 50 cm, and 70 cm are 02 DEC, 15 DEC, 16 DEC, 9 JAN and 23 JAN, respectively (Fig. 4). At 10 cm, 20 cm and 30 cm below surface, there is a sharp decrease in liquid water content when the soil temperature drops to 0 ℃, while at 50 cm and 70 cm below surface, due to freezing-induced water migration toward the freezing front, there is a gradual decrease in liquid water content before reaching a temperature of 0 ℃. At 90 cm below surface, probably because the freezing front is close enough to the sensor, although the temperature at the sensor does not reach 0 ℃, there is a significant decrease in liquid water content on 29 FEB due to freezing-induced water ~~migration~~redistribution. Therefore, the relationship between temperature and liquid water content recorded by 5TM sensors, which are based on the frequency domain reflectometer (FDR) method, well reflects the effect of freezing on liquid water content.

Due to the rising air temperature in spring, soil temperature at 10 cm increased from below 0 ℃ to above 0 ℃ on 1 MAR, which is considered to be the start of the thawing stage in the current study. Because the water level is highest on 1 APR as a result of the downward infiltration of thawed water, 1 APR is considered to be the end of the thawing period. For the ~~four~~ sensors at ~~10 cm,~~ 20 cm, 30 cm and 50 cm, the start dates of thawing stage are ~~1 MAR,~~ 2 MAR, 3 MAR, and 5 MAR, while for the sensor at 70 cm, the start date of thawing stage is 2 MAR, implying the occurrence of bi-directional thawing. Different from the quick response of soil temperature to freezing, the response of soil temperature to thawing is a slow process. For the 3 sensors at 10 cm, 20 cm and 30 cm, the duration from start to end of thawing is 13 days, while for the 2 sensors at 50 cm and 70 cm, the durations from start to end of thawing are 18 days and 26 days, respectively. ~~The thawing of frozen soil is accompanied by a trend of increasing liquid water content.~~ The liquid water content increases sharply at the end of thawing and is much higher than that before freezing~~, indicating~~ as a result of the contribution of freezing-induced water gain.

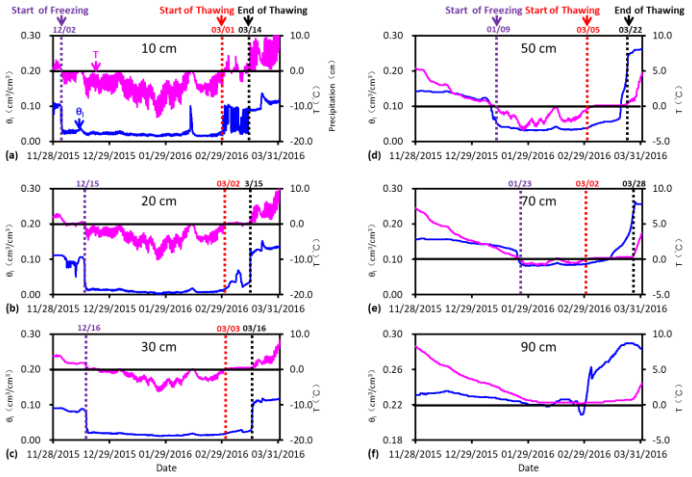

Figure 4 The observed hourly liquid water content and soil temperatures during the freezing-thawing cycle from 28 NOV 2015 to 1 APR 2016.

As shown in Fig. 1, water table depths on 28 NOV and 1 APR are 115 cm and 90 cm, respectively. Because snowfall in winter is ~~limited~~only 11.7 mm, the much higher water level at the end of thawing stage is mainly due to the occurrence of lateral groundwater inflow as reported in Jiang et al. (2017). The lowest water level equaling 143 cm below surface occurs on 29 JAN. ~~From 29 JAN, there is a~~The trend of rising water level from 29 JAN to 29 FEB, when frozen soil has not been thawed yet~~, which is one month earlier than the occurrence of thawed water infiltration during the thawing stage. This phenomenon can also be~~, is attributed to lateral groundwater inflow. The occurrence of lateral groundwater inflow also alleviated the magnitude of freezing-induced groundwater level decline from 28 NOV to 29 JAN, i.e., freezing-induced groundwater level decline should be greater than 28 cm. To quantify the water budget during the freezing/thawing cycle, ~~the abovementioned~~ we construct a model ~~is constructed~~ to determine the fluxes of freezing-induced migration, lateral groundwater flow, infiltration and soil evaporation.

3.2 ~~Freezing-induced~~ Numerical results of water redistribution ~~and evaporation during the freezing-thawing cycle: the effect of lateral groundwater flow and soil heterogeneity~~

Based on the parameters ~~of van Genuchten (1980) and Mualem (1976) equation~~ listed in Table ~~1~~2, and ~~the~~ with a lateral groundwater inflow rate of 1.03 mm/d, there are good fits between simulated and measured liquid water content in the frozen zone (Fig. 5a), ~~and also for~~and between simulated and measured soil temperature (Fig.

5b), as well as between simulated and measured ~~and~~ groundwater level (Fig. 6a). Fig. 5a also shows the simulated total water content, which coincides with liquid water content before freezing, but increases rapidly due to freezing-induced water migration from the underlying soil and finally maintains at a stable value corresponding to the completely frozen state.

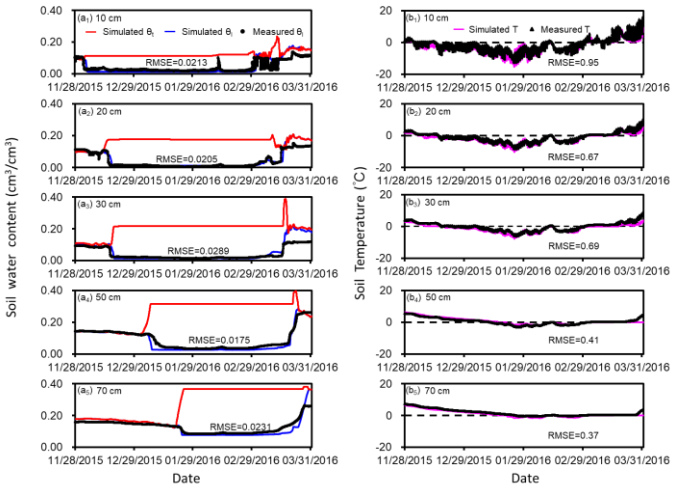

Figure 5 The observed and simulated liquid water content and simulated total water content (θ_t) (a_1-a_5) and soil temperature (b_1-b_5) at the 5 different depths within the frozen zone during the freezing-thawing cycle. The RMSEs of liquid water content and soil temperature are also listed.

Fig. 6 ~~(~~a~~)~~ shows the distribution of simulated soil temperature and frost depth. There is a good match between simulated and measured frost depth, the latter of which is determined by the dates of start of freezing and end of thawing as shown in Figure 4. In the frozen zone, as the frost depth increases, ~~the magnitude of increase in total water~~ ice content increases from the shallow to the deep, but liquid water content is generally maintained around the residual water content (Fig. 6b,c~~d~~). In the node above the frost depth, because the negative temperature is close to 0℃, the liquid water content is higher than the residual water content, while the ice content is lower than the overlying node. Note that when the frost depth reaches the middle layer with finer soils, there is a ~~larger~~thicker zone with lower ice content and higher liquid water content, which is related to the higher residual water content of the middle layer. In the whole frozen zone ~~except for the shallowest layer, the total water content at the end of the freezing stage is larger than that before freezing, and,~~ there ~~is a~~ trend of depth-increasing total water content toward the water table (Fig. 6d), ~~–~~ indicates a trend of depth-increasing water gain ~~indicating that the distance to the water table not only controls the initial liquid water content, but also the~~

~~amount of freezing-induced water gain from underlying soils~~controlled by the distance between the freezing front and the water table.

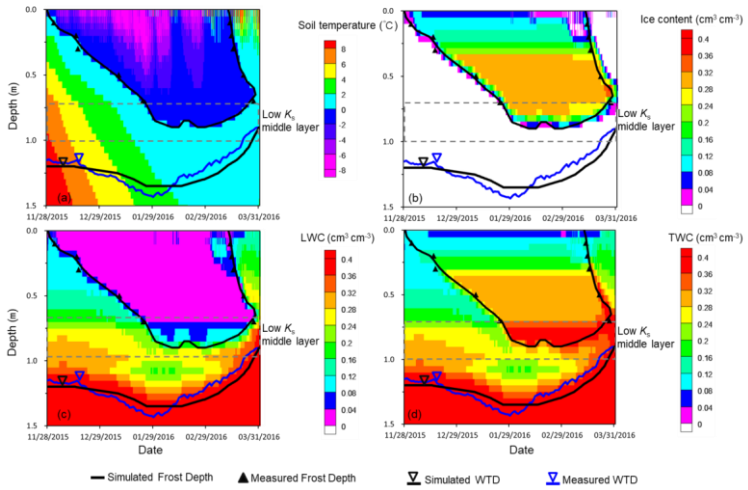

Figure 6 The evolution of simulated soil temperature (a), ice content (b), liquid water content (LWC) (c) and total water content (TWC) (d) at the field site. Also shown in the figures are evolutions of frost depth and groundwater level.

~~Soil texture and the corresponding hydraulic conductivity are also factors controlling the flux of freezing-induced water migration through the unfrozen zone. Because the soil texture in the layer from 70 cm to 100 cm is slightly different from overlying and underlying soils, we compare the distribution of total water content under the homogeneous case (Scenario B, Fig. 6b) with that of the base case (Scenario A, Fig. 6a). We find the low K_s of the middle layer restricts water migration into the part of frozen zone overlying the middle layer. As shown in Table 3, the increase of total water content in the frozen zone is 0.126 for Scenario B (corresponding to an increased water storage of 119.7 mm), and is 0.106 for Scenario A (corresponding to an increased water storage of 96.1 mm). Scenario A also has a smaller magnitude of freezing-induced water table decline (Table 3). Moreover, due to the ability of clay to retain more water, before late January when the frost depth is still away from the middle layer, the middle layer shown in Fig. 6a has more liquid water than that shown in Fig. 6b; from late January to late February when the freezing front in Fig. 6a is shallower than the bottom of the middle layer, the unfrozen part of the middle layer also has higher water content than the underlying soil.~~

~~Table 3 A comparison of water table decline (AWTD), frost depth (FD), and water gain in the frozen zone under~~

different groundwater conditions.

Groundwater conditions	Heterogeneous (low *Ks* middle layer)					Homogeneous				
	AWTD (mm)	FD (cm)	ΔS_{rz} (mm)	ΔTWC	Mean TWC	AWTD (mm)	FD (cm)	ΔS_{rz} (mm)	ΔTWC	Mean TWC
Fixed WTD=1.2 m	0	90	114.5	0.127	0.283	0	95	142.8	0.150	0.304
LFR=1.03 mm/d	15	90	96.1	0.106	0.265	30	95	119.7	0.126	0.282
LFR=0 mm/d	40	95	67.3	0.071	0.236	55	100	94.1	0.094	0.256

ΔSFZ represents increased water storage in the frozen zone, ΔTWC represents increased total water content in the frozen zone, and Mean TWC represents the mean total water content in the frozen zone at the state of completely frozen.

Figure 7 The temporal variations of simulated water table depth under different lateral groundwater inflow rates.

3.3 Soil evaporation during the freezing-thawing cycle

3.3 Water budgets during the freezing/thawing cycle: implications for appropriate boundary conditions

By comparing model results with and without consideration of the three snowfall events, we find snowfall did not infiltrate into the soil column due to the low permeability of frozen soil and got evaporated directly, implying that s

Infiltration of snowmelt and lateral groundwater inflow are two processes of water gain in the soil column, while soil Soil water evaporation is the only form of water loss leaving the top of the soil column during the freezing-thawing cycle. At our field site, the cumulative infiltration of snowmelt is simulated to be 3.2 mm, while the cumulative evaporation is simulated to be 32.0 mm, both of which are restricted by the frozen soil. Therefore, we use the evaporation rate without considering snowfall events to represent actual soil evaporation. Note that although snowfall is not considered, the atmospheric conditions associated with the snowfall event on 13 FEB still result in higher evaporation rate (Fig. 8). Based on the temporal trend evolution of evaporation rate versus

带格式的: 字体: (默认) Times New Roman, (中文) AdvOT46dcae81, 10 磅, 字体颜色: 自动设置

带格式的: 字体: (中文) AdvOT46dcae81, 10 磅, 字体颜色: 自动设置, 非上标/ 下标

带格式的: 行距: 2 倍行距

带格式的: 字体: (中文) AdvOT46dcae81, 10 磅, 字体颜色: 自动设置

带格式的: 字体: (中文) AdvOT46dcae81, 10 磅

带格式的: 字体: (默认) Times New Roman, (中文) AdvOT46dcae81, 10 磅, 字体颜色: 自动设置

带格式的: 字体: (中文) AdvOT46dcae81, 10 磅, 字体颜色: 自动设置

带格式的: 字体: (中文) AdvOT46dcae81, 10 磅

带格式的: 字体: (中文) AdvOT46dcae81, 10 磅, 字体颜色: 自动设置

带格式的: 字体: (默认) Times New Roman, (中文) AdvOT46dcae81, 10 磅, 字体颜色: 自动设置

带格式的: 字体: (中文) AdvOT46dcae81, 10 磅, 字体颜色: 自动设置

带格式的: 字体: (中文) AdvOT46dcae81, 10 磅

~~time~~(Fig. 7), we identify three stages of soil water evaporation. Stage Ⅰ has a trend of decreasing evaporation rate, stage Ⅱ has a limited evaporation rate, and stage Ⅲ has a trend of increasing evaporation rate. Note that in stage Ⅱ the atmospheric conditions associated with the snowfall event on 13 FEB result in slightly higher evaporation rate. ~~In both scenarios, the start of stage Ⅱ corresponds to a frost depth of around 20 cm. In Scenario A, the~~ The mean evaporation rates in the three stages are 0.36, 0.18 and 0.59 mm/d, respectively. ~~(Fig. 8a), leading to a cumulative evaporation of 32.0 mm; in Scenario B, the mean evaporation rates in the three stages are 0.53, 0.21 and 1.55 mm/d (Fig. 8b), respectively, corresponding to a cumulative evaporation of 55.3 mm.~~ Similar three stages of temporal evolution of soil evaporation during the freezing-thawing cycle have been reported in several field studies (Kaneko et al., 2006;Wu et al., 2016;Xue et al., 2020). The high evaporation in stage Ⅲ, which is a direct result of accumulation of liquid water during the thawing stage, well explains the occurrence of soil salinization in spring in many regions of the world (Liu et al., 2009;Lopez et al., 2010;Bechtold et al., 2011) .

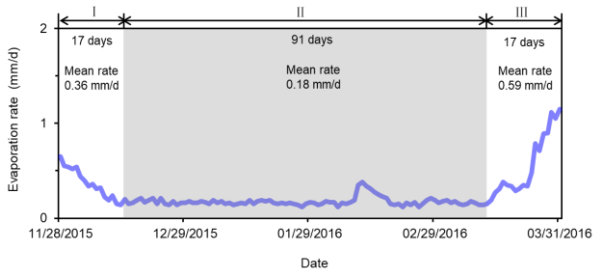

Figure ~~7~~8 The simulated daily soil evaporation rate at the field site ~~for Scenario A (a) and Scenario B (b)~~. Also shown ~~is~~ are the mean evaporation rates for ~~each~~ the three stages with different trends of daily soil evaporation rates.

~~In subsect. 3.2, based on the difference of total water content between the beginning and the end of the freezing stage, the increased water storage in the frozen zone induced by freezing was calculated to be 96.1 mm for Scenario A, and 119.7 mm for Scenario B. Considering the amount of water loss leaving the soil column due to soil evaporation, the actual cumulative freezing-induced water migration into the frozen zone should be 115.6 mm for Scenario A and 146.0 mm for Scenario B. Therefore, a clear quantification of soil evaporation is critical to understanding interactions of soil water and groundwater induced by freezing.~~

~~Because almost all Infiltration of snowmeltsnowfall are evaporated without entering the subsurface, soil evaporation and lateral groundwater inflow are the only twothree processes influencing the balance of water in~~

~~the soil column.~~ If the freezing/thawing cycle is divided into the freezing stage and the thawing stage, the balance of water in each stage can be written as

$$S_{s0} + S_{u0} + q \cdot \Delta t_F + I_F = S_{s1} + S_{u1} + ET_F \cdot \quad (10a)$$

$$S_{s1} + S_{u1} + q \cdot \Delta t_T + I_T = S_{s2} + S_{u2} + ET_T \cdot \Delta t_T \quad (10b)$$

where S_{s0} [L], S_{s1} [L] and S_{s2} [L] are cumulative water storages in the saturated zone at the beginning of freezing stage, at the end of freezing stage (beginning of thawing stage) and at the end of the thawing stage, respectively; S_{u0} [L], S_{u1} [L] and S_{u2} [L] are cumulative water storages in the unsaturated zone at the beginning of freezing stage, at the end of freezing stage (beginning of thawing stage) and at the end of the thawing stage, respectively; q [L/T] is the mean rate of lateral groundwater inflow during the freezing/thawing cycle; Δt_F [T] and Δt_T [T] are the durations of the freezing and thawing stages, respectively; I_F [L] and I_T [L] are the cumulative snowmelt infiltration during the freezing and thawing stages, respectively; ET_F [L/T] and ET_T [L/T] are the mean soil evaporation rates during the freezing and the thawing stages, respectively. The values of each term in Eq. (~~8~~10) are listed in Table 4.

~~Stage~~	~~Duration~~	~~Δt (d)~~	~~Initial S_s (mm)~~	~~Initial S_u (mm)~~	~~$q \cdot \Delta t$ (mm)~~	~~$ET \cdot \Delta t$ (mm)~~	~~Final S_s (mm)~~	~~Final S_u (mm)~~
~~Freezing~~	~~28 NOV 2015 - 28 FEB 2016~~	~~93~~	~~120.9~~	~~246.4~~	~~95.8~~	~~19.5~~	~~80.6~~	~~362.9~~
~~Thawing~~	~~29 FEB 2016 - 1 APR 2016~~	~~32~~	~~80.6~~	~~362.9~~	~~33.0~~	~~12.6~~	~~239.6~~	~~224.4~~

Table 4 Water budgets during the freezing-thawing cycle

Stage	Duration	Initial S_s (mm)	Initial S_u (mm)	$q \cdot \Delta t$ (mm)	I (mm)	$ET \cdot \Delta t$ (mm)	Final S_s (mm)	Final S_u (mm)	ΔS_s (mm)
Freezing	28 NOV 2015 - 28 FEB 2016 (93 days)	120.9	246.4	95.8	3.2	19.5	80.6	366.2	-136.1
Thawing	29 FEB 2016 - 1 APR 2016 (32 days)	80.6	366.2	33.0	0	12.5	239.6	227.7	126.0

Apparently, the change in groundwater ~~loss~~ storage, ΔS_s, during the freezing stage ~~is~~ can be calculated by $S_{s1} - S_{s0}$, which equals -40.3 mm and corresponds to a water table decline of 10 cm. In fact, such a water table decline has been alleviated by the lateral groundwater inflow. The change in groundwater storage, ΔS_s, ~~freezing-induced groundwater loss~~ should be calculated by S_{s1}-S_{s0}-$q \cdot \Delta t_F$, which equals -136.1 mm, i.e., -

freezing-induced groundwater loss should be 136.1 mm. In a groundwater flow model without considering the unsaturated zone, this process can be characterized by a mean upward groundwater flux of 1.46 mm/d with a duration of 93 days at the upper boundary. ~~Similarly, i~~ In the thawing stage, the change in groundwater storage, ΔS_s, ~~groundwater gain from downward infiltration~~ should be calculated by $S_{s2} - S_{s1} - q \cdot \Delta t_T$, which equals 126.0 mm. In a groundwater flow model, this process can be characterized by a mean downward groundwater flux of 3.94 mm/d at the upper boundary with a duration of 32 days.

As demonstrated in pioneering studies of regional groundwater flow (Hubbert, 1940; Toth, 1962) without considering the process of freezing-induced water redistribution, shallow groundwater in the discharge area is dominated by upward flow due to strong evapotranspiration. ~~This is consistent with the dominance of upward flux at the upper boundary in the unfrozen period at the study site (Jiang et al., 2017). Therefore, t~~The ~~current study~~above calculation confirms that during 3/4 of the freezing-thawing period, shallow groundwater ~~in the discharge area of a semi-arid catchment~~ is also dominated by upward flow~~, which is consistent with the direction of regional groundwater flow in the discharge area (Hubbert, 1940; Toth, 1962).~~ As demonstrated in Jiang et al. (2017), at our study site in the unfrozen period, the stage from late SEP 2014 to early OCT 2014 (with a duration of 18 days) is the only stage with ~~net infiltration in our study site, and the~~ net downward groundwater flux ~~equals~~ equaling 2.99 mm/d in our study site. The current study indicates that the thawing stage has an even larger downward groundwater flux and an even longer duration. Therefore, it is interesting to examine the pattern of two-dimensional or three-dimensional groundwater flow induced by the freezing-thawing cycle by using a fully coupled soil-groundwater freeze-thaw model in the future.

3.4 The effect of water table depth and lateral groundwater inflow on freezing-induced water redistribution

In Subsect.3.1, we inferred that due to the occurrence of lateral groundwater inflow, freezing-induced groundwater level decline is alleviated, and there is a trend of groundwater level rise before the end of the freezing stage. ~~Lateral groundwater flow is a component of water budget influencing water level.~~ Figure 8a shows the evolutions of total soil water content, frost depth and groundwater level under four conditions of groundwater inflow when the initial water table depth (WTD_0) equals 120 cm. When there is no lateral groundwater inflow (Fig. 8a1), the lowest water level occurs at the end of the freezing period, corresponding to a water table ~~depth~~ decline of 45 cm. ~~When there is no lateral groundwater flow, in either the heterogeneous case (Scenario C, Fig. 6c) or the homogeneous case (Scenario D, Fig. 6d), the lowest water level occurs at the end of~~

~~the freezing stage. By comparing the simulated groundwater level under a series of lateral groundwater inflow rates, we find the occurrence of lateral groundwater inflow alleviates the magnitude of freezing-induced water level decline, and~~A comparison of water table fluctuations under three different rates of lateral groundwater inflow (Fig. 8a1-a3) confirmed that ~~leads to a~~the trend of earlier water level rise before the start of the thawing stage is caused by lateral groundwater inflow ~~(Fig. 7)~~. Therefore, in the field, whether the time of lowest water table corresponds to that of the end of the freezing period can be used to infer the existence of lateral groundwater inflow/outflow ~~can be determined by the earlier occurrence of groundwater level rise before the start of the thawing stage~~. ~~Due to the occurrence of lateral groundwater inflow, the rise in water level from late January to late February also restricts the frost depth to some extent (Table 3).~~ The higher water level caused by lateral groundwater flow would be beneficial for freezing-induced water migration towards the freezing front. As lateral groundwater inflow rate changes from 0 to 0.51 to 1.03 mm/d, the increase in water storage in the frozen zone changes from 108.3 mm to 112.4 mm to 125.6 mm, while ~~In the heterogeneous cases, the increase in total water content in the frozen zone is found to be 0.106 in Scenario A, but is only 0.071 in Scenario C without lateral groundwater flow; in the homogeneous cases, t~~the increase in total water content in the frozen zone ~~is found to be 0.126 in Scenario B, but is only 0.094 in Scenario D without lateral groundwater flow~~changes from 0.114 cm^3/cm^3 to 0.118 cm^3/cm^3 to 0.132 cm^3/cm^3 (Table 5~~3~~). As shown in Fig. 8a3, the total water content above the freezing front could be as high as 0.286 cm^3/cm^3. We infer that the co-occurrence of shallow water table and lateral groundwater inflow would enhance the possibility of frost heave.~~Therefore, compared with scenarios without lateral groundwater inflow, the occurrence of lateral groundwater inflow can inevitably lead to an increased freezing-induced water accumulation. This confirms that a fixed head lower boundary condition would inevitably overestimate freezing-induced water migration. As we pointed out in the Introduction part, a fixed head lower boundary condition implies instantaneously replenishment of groundwater.~~

~~If a fixed head equaling 1.2 m below surface is assigned at the lower boundary, the increase in total water content in the frozen zone is 0.127 for the heterogeneous case, and is 0.150 for the homogeneous case (Table 3). The results shown in Fig. 7 indicate that an even larger groundwater inflow is needed to maintain a stable water level.~~

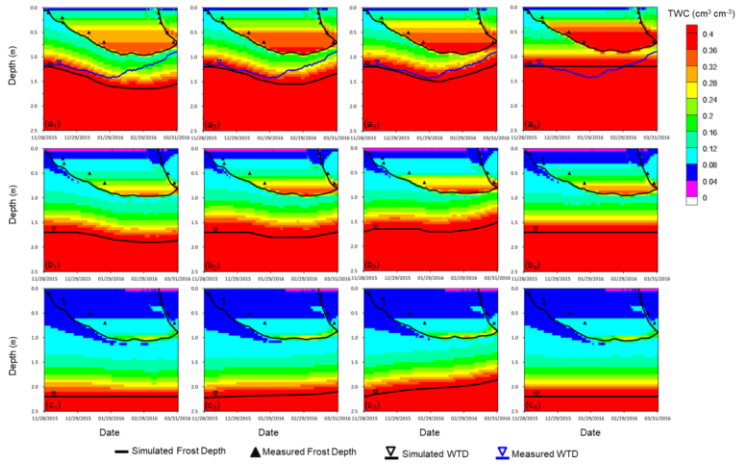

Figure 8 The evolutions of simulated total water content, frost depth and water table depth under three different initial water table depths (120 cm, 170 cm and 220 cm) and four different groundwater supply conditions.

Table 5 A comparison of water table decline (ΔWTD), frost depth (FD), and water gain in the frozen zone under different scenarios.

Scenarios	WTD_0 (cm)	ΔWTD (cm)	FD (cm)	Initial S_{FZ} (mm)	Final S_{FZ} (mm)	Mean TWC	ΔS_{FZ} (mm)	ΔTWC
Scenario A1	120	45	95	146.1	254.4	0.268	108.3	0.114
Scenario A2	120	35	95	146.1	258.5	0.272	112.4	0.118
Scenario A3	120	30	95	146.1	271.7	0.286	125.6	0.132
Scenario A4	120	-	90	130.6	274.4	0.305	143.8	0.160
Scenario B1	170	20	95	84.7	156.9	0.165	72.2	0.076
Scenario B2	170	10	95	84.7	161.9	0.170	77.2	0.081
Scenario B3	170	-5	95	84.7	177.6	0.187	92.9	0.098
Scenario B4	170	-	95	84.7	163.1	0.172	78.4	0.083
Scenario C1	220	0	105	79.4	102.0	0.097	22.6	0.022
Scenario C2	220	-5	105	79.4	102.8	0.098	23.4	0.022
Scenario C3	220	-20	105	79.4	105.4	0.100	26.0	0.025
Scenario C4	220	-	105	79.4	102.2	0.097	22.8	0.022
Scenario D	250	0	115	81.6	93.2	0.081	11.6	0.010

~~In Table 5, FD represents the maximum frost depth, the frozen zone represents the zone from the surface to FD.~~ Mean TWC ~~represents the mean total water content in the frozen zone at the state of completely frozen, which~~ is calculated by total water ~~content~~storage in the frozen zone (S_{FZ}) divided by ~~FD~~frost depth while~~.~~ ΔTWC, ~~represents increased total water content in the frozen zone, which~~ is calculated by increased water storage in the frozen zone (ΔS_{FZ}) divided by frost depth~~FD~~.

It is also interesting to examine the control of initial water table depth ~~(WTD_0)~~ on freezing-induced groundwater migration. Fig. 8b and 8c show the evolutions of total ~~soil~~ water content, frost depth and groundwater level when WTD_0 equals 170 cm and 220 cm. If there is no lateral groundwater inflow, freezing-induced groundwater level decline is 20 cm when WTD_0 equals 170 cm, and is 0 when WTD_0 equals 220 cm. Note that when WTD_0 equals 220 cm, there is still freezing-induced water migration from the unsaturated zone, the soil water content of which is supported by groundwater. When WTD_0 equals 250 cm, we find the lower soil water content below the freezing front led to an even smaller freezing-induced water migration, with the increased total water content equaling as low as 0.010 cm^3/cm^3 (Table 5). We also note that as WTD_0 increases, the smaller soil water content in the shallow part of the soil column also results in larger frost depths. When the lateral groundwater inflow is fixed at other rates, the increased water storage in the frozen zone also decreases with initial water table depth.

When the water table depth is fixed at 120 cm, 170 cm, and 220 cm, the increase in total water content in the frozen zone is found to be 0.160 cm^3/cm^3, 0.083 cm^3/cm^3 and 0.022 cm^3/cm^3, respectively. Compared with the cases without lateral groundwater inflow but with a dynamic water table (Scenarios A1, B1 and C1), a fixed water table leads to higher water gain in the frozen zone. This indicates that a fixed head lower boundary condition would overestimate freezing-induced water migration as well as the risk of frost heave because such a lower boundary condition implies instantaneously replenishment of groundwater. This comparison also shows the necessity of properly characterizing water table fluctuations induced by freezing and groundwater inflow/outflow.

4 Conclusions

Based on field observations of soil temperature, liquid soil water content and groundwater level at a site in the discharge area ~~of a catchment~~with shallow water table, it was found that the observed temporal variations of wintertime liquid water content and groundwater level are not only controlled by freezing and thawing, but also by lateral groundwater inflow. Therefore, we built a model ~~is built~~ to examine the responses of soil water and groundwater to wintertime climatic conditions and ~~occurrence of~~ lateral groundwater inflow. The observed fluctuating soil water contents and groundwater level induced by freezing and thawing are well reproduced by the calibrated model ~~in the saturated part of the soil column~~, which . ~~The calibrated model~~ increases our understanding of water balance as well as the influencing factors of freezing-induced water migration during the freezing-thawing cycle.

~~Our model results showed that almost all snowfall is evaporated without infiltrating into the soil column~~

~~due to the low permeability of frozen soil. Therefore, soil evaporation is the only form of water loss, while lateral groundwater inflow is the only source of water gain. We also found the middle layer with lower saturated hydraulic conductivity restricts both evaporation rates and freezing-induced water migration.~~

Based on the budget of groundwater during the freeing-thawing cycle, the mean flux of freezing-induced groundwater loss in the freezing stage with a duration of three months is 1.46 mm/d, and the mean flux of thawing-induced groundwater gain in the thawing stage with a duration of one month is found to be 3.94 mm/d. As found by Jiang et al. (2017), due to the semi-arid climate, the only stage with net recharge in the unfrozen period is from late September to early October. Therefore, combined with the fluxes obtained by Jiang et al. (2017) for the unfrozen period, the fluxes during the freeing-thawing cycle obtained in the current study can be useful for future transient groundwater flow models to characterize the control of climatic conditions on deeper groundwater flow in semi-arid regions with seasonally freezing and thawing processes. ~~By comparing models with and without lateral groundwater inflow, we found the occurrence of lateral groundwater inflow led to much smaller magnitude of freezing-induced water level decline and a trend of rising water level before the start of the thawing stage.~~

Based on a series of models with different initial water table depths ~~during the freezing-thawing cycle~~, we found that when water table depth is maintained at 220 cm below surface, although part of water in the unsaturated zone has been migrated to the freezing front, groundwater in the saturated zone is not directly involved in freezing-induced water migration. However, when initial water table depths are shallower than 220 cm, freezing-induced groundwater migration could be significant, and the rise in groundwater level due to lateral groundwater inflow could increase the amount of groundwater migrated to the freezing front. As reported in Fan et al., ~~(~~2013~~)~~, the regions with water table depth shallower than 2 m account for around 31% of the global land area, implying that the involvement of groundwater in freezing-induced water redistribution could be widespread. Although the threshold water table depth in other study areas with different climate conditions remains unknown, our study well demonstrated the necessity of properly characterizing freezing-induced water table fluctuations to quantify freezing-induced groundwater migration and its effect on engineering problems and ecological processes in cold regions.

Code/Data availability

The numerical models in the current study were built by using the SHAW model (vision 3.0), which is available at https://www.ars.usda.gov/pacific-west-area/boise-id/watershed-management-research/docs/shaw-model/.

The meteorological data of the Otak station is available from China Meteorological Data Service Center (http://data.cma.cn).

The observed soil temperature, liquid water content and water table depth from 28 NOV 2015 to 1 APR 2016 at the field site are available in the supplement document.

Author contribution

XJ designed the field site and HX was involved in data collection. All authors were involved in data interpretation. XJ and LW developed the initial idea of the current study, and HX established the models with inputs from all coauthors. HX and XJ wrote the manuscript with contributions from YZ.

Competing interests

The authors declare that they have no conflict of interest.

Acknowledgements

This study is supported by the National Natural Science Foundation of China (41772242), the Fundamental Research Funds for the Central Universities of China and the 111 Project (B20010). The authors thank two anonymous reviewers whose comments led to significant improvement of the study.

References

Alkhaier, F., Flerchinger, G. N., and Su, Z.: Shallow groundwater effect on land surface temperature and surface energy balance under bare soil conditions: modeling and description, Hydrology and Earth System Sciences, 16, 10.5194/hess-16-1817-2012, 2012.

Bechtold, M., Haber-Pohlmeier, S., Vanderborght, J., Pohlmeier, A., Ferre, A., and Vereecken.H: Near-surface solute redistribution during evaporation, Geophysical Research Letters, 38, 17404, 10.1029/2011GL048147, 2011.

Bronfenbrener, L., and Bronfenbrener, R.: Frost heave and phase front instability in freezing soils, Cold Regions Science and Technology, 64, 19-38, 10.1016/j.coldregions.2010.07.001, 2010.

Chamberlain, E. J.: Frost susceptibility of soil, review of index tests, Cold regoins research and engineering lab hanover NH, 1981.

Chen, J., Gao, X., Zheng, X., Miao, C., Zhang, Y., Du, Q., and Xu, Y.: Simulation of Soil Freezing and Thawing for Different Groundwater Table Depths, Vadose Zone Journal, 18:18057, 10.2136/vzj2018.08.0157, 2019.

Cherkauer, K. A., and Lettenmaier, D. P.: Hydrologic effects of frozen soils in the upper Mississippi River basin, Journal of Geophysical Research: Atmospheres, 104, 19599-19610, 10.1029/1999jd900337, 1999.

Daniel, J. A., and Staricka, J. A.: Frozen Soil Impact on Grounf Water - Surface Water Interaction, JAWRA Journal of the American Water Resources Association, 36, 151-160, 10.1111/j.1752-1688.2000.tb04256.x, 2000.

DeGaetano, A. T., Cameron, M. D., and Wilks, D. S.: Physical Simulation of Maximum Seasonal Soil Freezing Depth in the United States Using Routine Weather Observations, Journal of Applied Meteorology, 40, 546-555, 10.1175/1520-0450(2001)040<0546:psomss>2.0.co;2, 2001.

Demand, D., Selker, J. S., and Weiler, M.: Influences of Macropores on Infiltration into Seasonally Frozen Soil, Vadose Zone Journal, 18, 10.2136/vzj2018.08.0147, 2019.

~~Dobinski, W.: Permafrost, Earth-Science Reviews, 108, 158-169, 10.1016/j.earscirev.2011.06.007, 2011.~~

Drescher, W. J.: Some effects of preciptiation on ground water in Wisconsin, Wisconsin Geological Survey, 1955.

~~Evans, S. G., and Ge, S.: Contrasting hydrogeologic responses to warming in permafrost and seasonally frozen ground hillslopes, Geophysical Research Letters, 44, 1803-1813, 10.1002/2016gl072009, 2017.~~

Evans, S. G., Ge, S., Voss, C. I., and Molotch, N. P.: The role of frozen soil in groundwater discharge predictions for warming alpine watersheds, Water Resources Research, 54, 1599-1615, 10.1002/2017WR022098, 2018.

Fan, Y., Li, H., and Miguez-Macho, G.: Global patterns of groundwater table depth, Science, 339, 940-943, 10.1126/science.1229881, 2013.

Fetzer, Thomas, Vanderborght, Jan, Mosthaf, Klaus, Smits, Kathleen, M., Helmig, and Rainer: Heat and water transport in soils and across the soil-atmosphere interface: 2. Numerical analysis, Water resources research, 53, 1080-1100, 10.1002/2016WR019983, 2017.

Flerchinger, G. N., and Saxton, K. E.: Simultaneous heat and water model of a freezing snow-residue-soil system I. Theory and development, Transactions of the ASAE, 32, 565-0571, 10.13031/2013.31040, 1989.

Flerchinger, G. N.: The simultaneous heat and water (SHAW) model: user's manual, Technical Rep. NWRC, 10, 2000.

Fuchs, M., Campbell, G., and Papendick, R.: An Analysis of Sensible and Latent Heat Flow in a Partially Frozen Unsaturated Soil 1, Soil Science Society of America Journal, 42, 379-385, 10.2136/sssaj1978.03615995004200030001x, 1978.

Gleeson, T., Marklund, L., Smith, L., and Manning, A. H.: Classifying the water table at regional to continental scales, Geophysical Research Letters, 38, L05401, 10.1029/2010gl046427, 2011.

Hansson, K., and Lundin, L.-C.: Equifinality and sensitivity in freezing and thawing simulations of laboratory and in situ data, Cold Regions Science and Technology, 44, 20-37, 10.1016/j.coldregions.2005.06.004, 2006.

Harlan, R.: Analysis of coupled heat‐fluid transport in partially frozen soil, Water Resources Research, 9, 1314-1323, 10.1029/WR009i005p01314, 1973.

Hayhoe, H.: Field testing of simulated soil freezing and thawing by the SHAW model, Canadian Agricultural Engineering, 36, 279, 1994.

Hirota, T.: An extension of the force-restore method to estimating soil temperature at depth and evaluation for frozen soils under snow, Journal of Geophysical Research, 107, 4767, 10.1029/2001jd001280, 2002.

Hohmann, M.: Soil freezing — the concept of soil water potential. State of the art, Cold Regions Science & Technology, 25, 101-110, 10.1016/S0165-232X(96)00019-5, 1997.

Hou, G., Liang, Y., Su, X., Zhao, Z., Tao, Z., Yin, L., Yang, Y., and Wang, X.: Groundwater Systems and Resources in the Ordos Basin, China, Acta Geologica Sinica, 82, 1061-1069, 10.1111/j.1755-6724.2008.tb00664.x, 2010.

Hubert, M.: The Theory of Ground-Water Motion, Soil Science, 51, 428, 10.1097/00010694-194105000-00015, 1940.

Ireson, A. M., van der Kamp, G., Ferguson, G., Nachshon, U., and Wheater, H. S.: Hydrogeological processes in seasonally frozen northern latitudes: understanding, gaps and challenges, Hydrogeology Journal, 21, 53-66, 10.1007/s10040-012-0916-5, 2013.

Iwata, Y., Hayashi, M., and Hirota, T.: Comparison of snowmelt infiltration under different soil-freezing conditions influenced by snow cover, Vadose Zone Journal, 7, 79-86, 10.2136/vzj2007.0089, 2008.

Jiang, X.-W., Sun, Z.-C., Zhao, K.-Y., Shi, F.-S., Wan, L., Wang, X.-S., and Shi, Z.-M.: A method for simultaneous estimation of groundwater evapotranspiration and inflow rates in the discharge area using seasonal water table fluctuations, Journal of hydrology, 548, 498-507, 10.1016/j.jhydrol.2017.03.026, 2017.

Jiang, X. W., Wan, L., Wang, X. S., Wang, D., and Zhao, K. Y.: A multi-method study of regional groundwater circulation in the Ordos Plateau, NW China, Hydrogeology Journal, 1657-1668, 10.1007/s10040-018-1731-4, 2018.

Kahimba, F. C., Ranjan, R. S., and Mann, D. D.: Modeling soil temperature, frost depth, and soil moisture redistribution in seasonally frozen agricultural soils, Applied engineering in agriculture, 25, 871-882, doi: 10.13031/2013.29237, 2009.

Kaneko, T., Kobayashi, T., Wang, W., and Cho, H.: Estimating Evaporation in Winter at a Field Irrigated Late in Autumn in Inner Mongolia, China, Journal Faculty of Agriculture Kyushu University, 51, 407-411, 10.1017/S0021859605005733, 2006.

Kurylyk, B. L., MacQuarrie, K. T., and Voss, C. I.: Climate change impacts on the temperature and magnitude of groundwater discharge from shallow, unconfined aquifers, Water Resources Research, 50, 3253-3274, 10.1002/2013WR014588, 2014.

Li, Q., Sun, S., and Xue, Y.: Analyses and development of a hierarchy of frozen soil models for cold region study, Journal of Geophysical Research Atmospheres, 115, 10.1029/2009JD012530, 2010.

Li, W., Brunner, P., Franssen, H. J. H., Li, Z., Wang, Z., Zhang, Z., and Wang, W.: Potential evaporation dynamics over saturated bare soil and an open water surface, Journal of Hydrology, 590, 125140, 10.1016/j.jhydrol.2020.125140., 2020.

Liu, Q., Cui, B., and Yang, Z.: Dynamics of the soil water and solute in the sodic saline soil in the Songnen Plain, China, Environmental Earth ences, 59, 837-845, 10.1007/s12665-009-0079-4, 2009.

Lopez, C. M. L., Brouchkov, A., Nakayama, H., Takakai, F., Fedorov, A. N., and Fukuda, M.: Epigenetic salt accumulation and water movement in the active layer of central Yakutia in eastern Siberia, Hydrological Processes, 21, 103-109, 10.1002/hyp.6224, 2010.

Mualem, Y.: A new model for predicting the hydraulic conductivity of unsaturated porous media, Water resources research, 12, 513-522, 10.1029/WR012i003p00513, 1976.

Nelson, F. E.: (Un) frozen in time, Science, 299, 1673-1675, 10.1126/science.1081111, 2003.
Okkonen, J., Ala-Aho, P., Hänninen, P., Hayashi, M., Sutinen, R., and Liwata, P.: Multi-year simulation and model calibration of soil moisture and temperature profiles in till soil, European Journal of Soil Science, 68, 829-839, 10.1111/ejss.12489, 2017.
Romano, N., Brunone, B., and Santini, A.: Numerical analysis of one-dimensional unsaturated flow in layered soils, Advances in Water Resources, 21, 315-324, 10.1016/S0309-1708(96)00059-0, 1998.
Rui, D., Zhai, J., Li, G., Zhang, J., and Suzuki, T.: Field experimental study of the characteristics of heat and water transfer during frost heaving, Cold regions ence and technology, 168, 10.1016/j.coldregions.2019.102892, 2019.
Schaap, M. G., and Leij, F. J.: Database-Related Accuracy and Uncertainty of Pedotransfer Functions, Soil science, 163, 765-779, 10.1097/00010694-199810000-00001, 1998.
Schneider, R.: Correlation of ground-water levels and air temperatures in the winter and spring in Minnesota: US Geol, Survey Water-Supply Paper, 1962, 1961.
Schuur, E. A. G., Mcguire, A. D., Sch?Del, C., ., Grosse, G., ., Harden, J. W., Hayes, D. J., Hugelius, G., ., Koven, C. D., Kuhry, P., ., and Lawrence, D. M.: Climate change and the permafrost carbon feedback, Nature, 520, 171-179, 2015.
Shoop, S. A., and Bigl, S. R.: Moisture migration during freeze and thaw of unsaturated soils: modeling and large scale experiments, Cold Regions Science & Technology, 25, 33-45, 10.1016/S0165-232X(96)00015-8, 1997.
Stähli, M., Jansson, P.-E., and Lundin, L.-C.: Soil moisture redistribution and infiltration in frozen sandy soils, Water Resources Research, 35, 95-103, 10.1029/1998wr900045, 1999.
Stephens, D.: Vadose zone hydrology, Lewis, Baca Raton, FL, 1996.
Tóth, J.: A theory of groundwater motion in small drainage basins in central Alberta, Canada, Journal of Geophysical Research, 67, 4375-4388, 10.1029/JZ067i011p04375, 1962.
Van Dam, J., and Feddes, R.: Numerical simulation of infiltration, evaporation and shallow groundwater levels with the Richards equation, Journal of Hydrology, 233, 72-85, 10.1016/S0022-1694(00)00227-4, 2000.
van der Kamp, G., Hayashi, M., and Gallén, D.: Comparing the hydrology of grassed and cultivated catchments in the semi-arid Canadian prairies, Hydrological Processes, 17, 559-575, 10.1002/hyp.1157, 2003.
van Genuchten, M. T.: A closed-form equation for predicting the hydraulic conductivity of unsaturated soils 1, Soil Science Society of America Journal, 44, 892-898, 10.2136/sssaj1980.03615995004400050002x, 1980.
Vanderborgh, J., Fetze, T., Mostha, K., Smit, K. M., and Helmi, R.: Heat and water transport in soils and across the soil-atmosphere interface: 1. Theory and different model concepts, Water Resources Research, 53, 1057-1079, 10.1002/2016WR019982, 2017.
Walvoord, M. A., and Kurylyk, B. L.: Hydrologic Impacts of Thawing Permafrost—A Review, Vadose Zone Journal, 15, 10.2136/vzj2016.01.0010, 2016.
Wang, J. Z., Jiang, X. W., Wan, L., Worman, A., Wang, H., Wang, X. S., and Li, H.: An analytical study on artesian flow conditions in unconfined‐aquifer drainage basins, Water Resources Research, 51, 8658-8667, 10.1002/2015WR017104, 2015.
Wexler, A., Hyland, R., and Stewart, R.: Thermodynamic properties of dry air, moist air and water and SI psychrometric charts, ASHRAE, 1983.
Williams, P., and Smith, M.: The frozen earth: fundamentals of geocryology, Cambridge University Press, 1989.
Willis, W. O., Parkinson, H. L., Carlson, C. W., and Haas, H. J.: Water table changes and soil moisture loss under frozen conditions, Soil science, 98, 244-248, 10.1097/00010694-196410000-00005, 1964.
Wu, M., Huang, J., Wu, J., Tan, X., and Jansson, P.-E.: Experimental study on evaporation from seasonally frozen soils under various water, solute and groundwater conditions in Inner Mongolia, China, Journal of Hydrology, 535, 46-53, 10.1016/j.jhydrol.2016.01.050, 2016.

Xue, J., Feng, H., Chen, J., Zheng, X., and Du, Q.: The Effect of a Sand Interlayer on Soil Evaporation during the Seasonal Freeze–Thaw Period in the Middle Reaches of the Yellow River, Water, 12, 2092, 10.3390/w12082092, 2020.

Xue, K., Wen, Z., Zhu, Z., Wang, D., and Zhang, M.: An experimental study of the relationship between the matric potential, unfrozen water, and segregated ice of saturated freezing soil, Bulletin of Engineering Geology and the Environment, 80(3), 10.1007/s10064-020-02052-x, 2021.

Yang, K., Qin, J., Zhao, L., Chen, Y., Tang, W., Han, M., Chen, Z., Lv, N., Ding, B., Wu, H., and Lin, C.: A multiscale soil moisture and freeze-thaw monitoring network on the third pole, Bulletin of the American Meteorological Society, 94(12), 1907-1916, 10.1175/BAMS-D-12-00203.1, 2013.

Yorukoglu, M., and Celik, A. N.: A critical review on the estimation of daily global solar radiation from sunshine duration, Energy Conversion & Management, 47, 2441-2450, 10.1016/j.enconman.2005.11.002, 2006.

Yu, L., Zeng, Y., Wen, J., and Su, Z.: Liquid‐Vapor‐Air Flow in the Frozen Soil, Journal of Geophysical Research: Atmospheres, 123, 7393-7415, info:doi/10.1029/2018JD028502, 2018.

Yu, L., Zeng, Y., and Su, Z.: Understanding the mass, momentum, and energy transfer in the frozen soil with three levels of model complexities, Hydrology and Earth System Sciences, 24, 4813-4830, 10.5194/hess-24-4813-2020, 2020.~~Zhang, T., Barry, R., Knowles, K., Ling, F., and Armstrong, R.: Distribution of seasonally and perennially frozen ground in the Northern Hemisphere, Proceedings of the 8th International Conference on Permafrost, 2003, 1289-1294,~~

Zhang, Y., Cheng, G., Li, X., Jin, H., Yang, D., Flerchinger, G. N., Chang, X., Bense, V. F., Han, X., and Liang, J.: Influences of Frozen Ground and Climate Change on Hydrological Processes in an Alpine Watershed: A Case Study in the Upstream Area of the Hei'he River, Northwest China, Permafrost and Periglacial Processes, 28, 420-432, 10.1002/ppp.1928, 2017.

Zhang, Y, Schaap, M. G., and Marcel, G.: Weighted recalibration of the Rosetta pedotransfer model with improved estimates of hydraulic parameter distributions and summary statistics (Rosetta3), Journal of Hydrology, 547, 39-53, 10.1016/j.jhydrol.2017.01.004, 2017.

Zhang, Z., Wang, W., Gong, C., Wang, Z., Duan, L., Yeh, T. c. J., and Yu, P.: Evaporation from seasonally frozen bare and vegetated ground at various groundwater table depths in the Ordos Basin, Northwest China, Hydrological Processes, 10.1002/hyp.13404, 2019.

Zhao, K. Y., Jiang, X. W., Wang, X. S., and Wan, L.: Restriction of groundwater recharge and evapotranspiration due to a fluctuating water table: a study in the Ordos Plateau, China, Hydrogeology Journal, 2, 1-11, 10.1007/s10040-020-02208-9, 2020.

Zhu, Y. , Ren, L. , Skaggs, T. H. , Lue, H. , Yu, Z. , and Wu, Y. , Fang, X. Q.: Simulation of populus euphratica root uptake of groundwater in an arid woodland of the ejina basin, china. Hydrological Processes, 23(17), 2460-2469, 10.1002/hyp.7353, 2010